HIGH RESOLUTION TIME-FREQUENCY DISTRIBUTIONS FOR MANEUVERING TARGET DETECTION IN OVER-THE-HORIZON RADARS

Yimin Zhang[†], *Moeness G. Amin*[†], *and Gordon J. Frazer*[‡]

[†] Center for Advanced Communications
Villanova University, Villanova, PA 19085, USA
E-mail: yimin@ieee.org, moeness@ece.villanova.edu

[‡] ISR Division, DSTO Edinburgh, Australia
E-mail: frazer@ieee.org

ABSTRACT

A novel high-resolution time-frequency representation method is proposed for source detection and classification in over-the-horizon radar (OTHR) systems. A data-dependent kernel is applied in the ambiguity domain to capture the target signal components, which are then resolved using the root-MUSIC based coherent spectrum estimation. This method is particularly effective to analyze a multi-component signal with time-varying time-Doppler signatures. By using the different time-Doppler signatures embedded in the multipath signals, this proposed method can reveal important target maneuvering information, whereas other linear and bilinear time-frequency representation methods fail.

1. INTRODUCTION

By exploiting the reflective and refractive nature of high-frequency (HF) radiowave propagation through the ionosphere, over-the-horizon radars (OTHRs) perform wide-area surveillance at long range well beyond the limit of the horizon of conventional line-of-sight (LOS) radars [1, 2, 3].

A significant problem in OTHR is robust high-resolution Doppler processing of accelerating or decelerating targets. This arises during aircraft and ship target maneuver and during observations of rockets during boost phase and mid-course flight. The complex Doppler signatures present in these cases reveal important information about the target.

Most OTHR systems use classical Doppler processing where one Doppler spectrum is computed using one full coherent integration time (CIT). Some systems use overlapped Doppler processing to provide a spectrogram analysis of time-varying Doppler. Accelerating/decelerating targets smear in Doppler and have reduced detectability and localization. The smearing reduces resolution and can obscure important multi-component Doppler features.

There are numerous time-frequency distributions (TFDs) other than the spectrogram [4, 5]. Many TFDs provide superior localization in time and Doppler frequency. Previous applications of time-frequency signal representations to OTHR, however, have generally been disappointing. The fundamental challenge and demand in OTHR is that TFD must retain its desirable resolution and concentration properties in the presence of clutter that is typically 40dB or more stronger than the target (although possibly localized in a different region of time-Doppler).

The objective of this paper is to investigate and extend recent developments in data-dependent TFDs to the problem of robust high-resolution analysis of time-varying OTHR target returns. Of particular interest is the problem of multi-component target signal detection and identification where important information of the maneuvering targets should be revealed. Such information is of significant value for the classification of the targets and the prediction of ballistic destinations.

2. SIGNAL MODEL

The received OTHR signal, after waveform dechirping at the receiver, is expressed as

$$y(t) = x(t) + u(t), \tag{1}$$

where $x(t)$ is the return signal from the target, and $u(t)$ is the clutter which also includes the additive noise.

In a typical OTHR scenario, in addition to the path directly reflected from the ionosphere, there is a multipath due to additional reflection from the ground or

This work is supported by the Office of Naval Research under Grant No. N00014-98-1-0176.

sea near the target. Denote l_1 and l_2 as the propagation distance of the two paths, respectively, and d_t and d_r as the respective one-way slant range between the transmitter and the target and between the target and the receiver, respectively. Then, d_t takes the value of either l_1 and l_2 and so does d_r.[1] Therefore, the received signal consists of four combination paths which result in the following three multipath components:

$$x(t) = A_1 e^{-j\omega 2l_1/c} + A_2 e^{-j\omega 2l_2/c} + A_3 e^{-j\omega(l_1+l_2)/c}, \quad (2)$$

where c denotes the speed of light, $\omega = 2\pi f_c$ is the carrier radian frequency, and A_1, A_2, and A_3 are the corresponding path losses.

In this paper, we consider a well encountered scenario of a maneuvering aircraft as an example. In this case, the target makes a 180^{O} turn in $T = 30.72$ seconds to change the height and direction. This time interval corresponds to 6 revisits (blocks), and each block contains 256 samples. The parameters used in the analysis and simulations are listed in Table 1. All the multipath signals are considered to fall in the same range cell. The time-Doppler signatures is plotted in Fig. 1. The dominant Doppler component is proportional to the target velocity in the slant range direction, and the small Doppler difference between the three paths is proportional to the ascending velocity of the target. The Doppler difference between the three paths, therefore, reveals important information on how the target moves in the elevation direction. The maximum one-side Doppler difference corresponding to the maximum ascending speed 1500 m/min = 25 m/s is about 1.17 Hz.

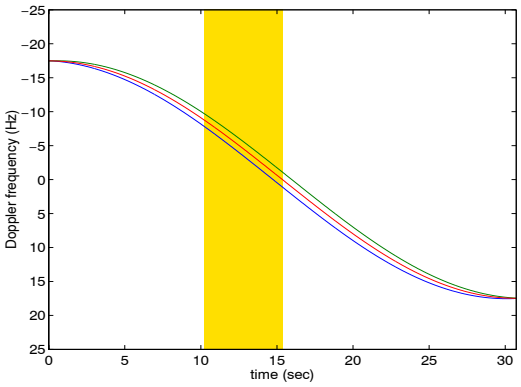

Figure 1: Time-Doppler signature (block 3 is colored).

[1] A backscattering OTHR system uses different transmitter and receiver antennas located at different places. Therefore, the range of a target is slightly different when viewed from the transmitter and the receiver. However, without loss of generality, we assume identical values for notation simplicity.

Table 1: Major Parameters

Parameter	Notation	Value
initial range	$R(0)$	2000 km
ionosphere height	H	350 km
aircraft initial height	$h(0)$	10000 m
maximum range speed	v	500 km/hr
maximum climbing speed	v_c	1500 m/min
carrier frequency	f_c	20 MHz
repetition frequency	f_s	50 Hz
samples per block	N	256 samples

3. CLUTTER SUPPRESSION

In this paper, we consider TFD methods to achieve high-resolution time-Doppler localization. In the underlying problem, TFDs are referred to as time-Doppler distributions (TDDs). The most commonly used TFD is the Wigner-Ville Distribution (WVD). The WVD of signal $y(t)$ is defined as

$$W_{yy}(t,f) = \int y(t+\tau/2)y^*(t-\tau/2)e^{-j\omega\tau} \quad (3)$$

where the superscript "*" denotes complex conjugate. All integrals without limits imply integration from $-\infty$ to $+\infty$. Substituting (1) in (3), the WVD of $y(t)$ can be written in terms of

$$W_{yy}(t,f) = W_{xx}(t,f) + W_{uu}(t,f) + W_{xu}(t,f) + W_{ux}(t,f), \quad (4)$$

where the first two terms are, respectively, the autoterms of the target signal and the clutter, and the other two are their crossterms. In a typical OTHR receiver, the clutter is much stronger than the target signal. Without substantial suppression of the clutter, the WVD autoterm of the target will be significantly obscured by the clutter autoterm as well as the crossterms between the clutter and signal.

We point to the fact that the clutter is highly localized in low frequencies and can be well modeled as an autoregressive (AR) process. Therefore, the clutter can be substantially suppressed by using the AR prewhitening techniques. Denote P as the order of the AR model, the AR polynomial parameters $a(t), t = 0, ..., P$ can be estimated via the modified covariance method [6].

Filtering the received signal $y(t)$ through a finite impulse filter (FIR), constructed using the AR polynomial parameters, results in the pre-whitened signal:

$$z(t) = y(t) * a(t) = z_x(t) + z_u(t), \quad (5)$$

where "*" denotes the convolution operator.

In this paper, the target signal modeled in Section 2 is overlayed on real OTHR clutter data. We assume that $A_1 = A_2$. The order of the AR model should be chosen to maximize the signal-to-clutter ratio (SCR). In this paper, the order of the AR model is set to a unit value (P=1). The spectrogram of block 3, which corresponds to the 256 samples from 10.24 to 15.36 seconds, before and after the AR pre-whitening is shown in Fig. 2. It is seen that, while the clutter is substantially suppressed by more than 40 dB, the target signal is only partially affected when its Doppler frequency is very close to that of the clutter. Fig. 3 shows the WVD of the pre-whitened data $z(t)$. While it is often difficult to identify the target in the WVD before pre-whitening, the target signature can be somewhat identified in Fig. 3. Further and key improvement in resolutions of the target signature components can be achieved by using the techniques highlighted in Section 4.

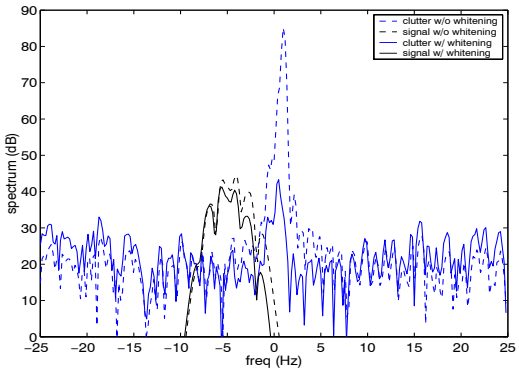

Figure 2: Block-wise spectrogram of the received signal before and after AR pre-whitening.

4. HIGH-RESOLUTION TIME-DOPPLER PROCESSING

To achieve chirp signal detection, discrimination, and classification, we propose time-Doppler estimation based on adaptive kernel and high-resolution time-Doppler localization.

4.1. Adaptive Kernel Design

In the following, each component of the signal return from the target is approximated as a chirp over the period of one block, i.e.,

$$x(t) = \sum_{i=1}^{3} A_i e^{j(\alpha_i t + \beta_x t^2/2)}. \qquad (6)$$

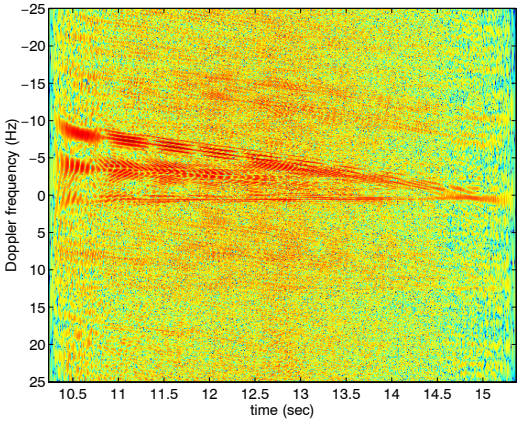

Figure 3: WVD of the received signal $z(t)$ after AR pre-whitening (block 3).

To estimate the chirp rate of the signal, it is common to exploit the ambiguity function. All ambiguity function autoterms pass through the origin, whereas the crossterms are often away from the origin. For a multi-component parallel chirp signal, the ambiguity function shows linear signatures depending on the signal chirp rate. The ambiguity function of $z(t)$ is defined as

$$A_z(\theta, \tau) = \int_t z(t + \tau/2) z^*(t - \tau/2) e^{j\theta t} dt \qquad (7)$$

where θ and τ are, respectively, the frequency-lag and time-lag variables. The chirp rate can be estimated by searching for the peaks of the following Q function [7]

$$Q(\xi) = \int |A_z(r\cos\xi, r\sin\xi)| dr. \qquad (8)$$

In the case considered, peaks possibly appear at $\xi_x = -1/\tan^{-1}(\beta_x)$ and $\xi_u = -1/\tan^{-1}(\beta_u)$, where β_x and β_u are the chirp rates of the signal and the principle component of the residual clutter, respectively.

Based on the chirp rate estimation, an adaptive kernel can be designed. We construct a kernel whose pass-band only captures the target signal chirp rate. The clutter will be, subsequently, mitigated in the ambiguity domain due to its disdinct orientations. For an estimated chirp rate $\hat{\xi}_x$, the following adaptive kernel is constructed to encompass the autoterm ambiguity function of the target signal, i.e.,

$$\phi_a(\theta, \tau) = e^{-d^2(\theta,\tau)/\sigma^2} \qquad (9)$$

where σ is the kernel width, and

$$d^2(\theta, \tau) = \theta^2 + \tau^2 - (\theta \sin\hat{\xi}_x + \tau\cos\hat{\xi}_x)^2. \qquad (10)$$

The adaptive kernel suppresses the clutter and noise, as well as all crossterms.

4.2. High Resolution Time-Doppler Localization

In [7], chirp MUSIC was introduced which estimates the Doppler frequencies at each time index t. The estimated auto-correlation function $\hat{R}_x(t,\tau)$ is used to constructed a data matrix for MUSIC spectrum estimation. However, the resulting matrix is, in general, not positive definite. Therefore, in [7], the filtered ambiguity function is transformed to the time-frequency domain, and only the positive part of the TFD is considered for the construction of the auto-correlation function. This method, although showing good time-Doppler localization in high signal-to-noise ratio (SNR) situations, is computationally inefficient because spectrum estimation is implemented for each time index. In addition, the estimated time-Doppler signature is not always consistent with the true values, particularly in low SNR scenarios. Therefore, it is difficult to be applied in the underlying OTHR systems.

In this paper, we obtain the auto-correlation directly from the filtered ambiguity function as

$$\hat{R}_x(t,\tau) = \frac{1}{2\pi}\int A_x(\theta,\tau)\phi_a(\theta,\tau)e^{-j\theta t}d\theta. \qquad (11)$$

Because signal components with single chirp rate are involved, the auto-corelation function $R_{x,i}(t,\tau)$ of each chirp component has the form

$$R_{x,i}(t,\tau) = A_i^2 e^{j(\alpha_i+\beta_x t)\tau}, \qquad (12)$$

which is dependent of t. Such dependence can be removed by using the estimated value, $\hat{\beta}_x = -1/\tan(\hat{\xi}_x)$. From $R_{x,i}(t,\tau)$, the time-independent auto-correlation function is estimated as

$$\tilde{R}_x(\tau) = \int \hat{R}_x(t,\tau)e^{-j\hat{\beta}_x t\tau}dt. \qquad (13)$$

The coherent integration yields coherent MUSIC subspace estimation of α_i's for improved performance. The vector $\tilde{R}_x(\tau)$ is considered as raw data sequence, rather than as covariance elements as in [7], to ensure the positive definiteness of the covariance matrix for spectrum estimation. In our simulations, root-MUSIC algorithm is used for computational convenience. Only one root-MUSIC operation is required for each block. The chirp signatures at different times are then constructed using the estimated chirp rate and α_i's.

In Fig. 4, the coherent time-varying MUSIC spectrum is shown for block 3. Despite the low SCR, the time-Doppler signatures, along with the Doppler frequency difference information, are estimated clearly and consistently. Simulation results for all other blocks also confirmed successful Doppler signature estimation.

5. CONCLUSION

In this paper, a novel method has been proposed for high-resolution time-Doppler signature localization applied to over-the-horizon radar systems. By combining AR pre-whitening for effective clutter suppression, time-frequency based signal discrimination, and coherent high-resolution spectrum analysis, the proposed method provides robust estimation of time-varying Doppler signature in low signal-to-clutter ratio (SCR) scenarios.

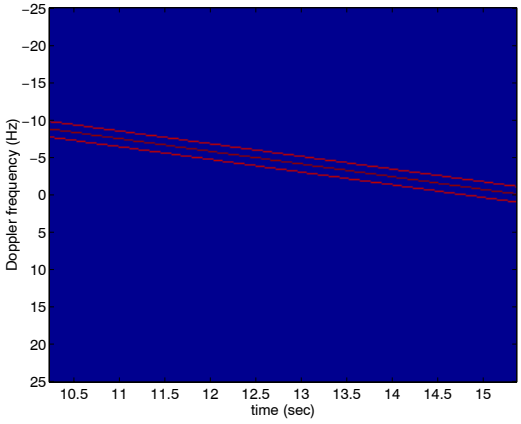

Figure 4: Coherent chirp MUSIC spectrum (block 3).

REFERENCES

[1] J. M. Headrick and M. I. Skolnik, "Over-the-horizon radar in the HF band," *Proc. IEEE*, vol. 62, pp. 664–673, 1974.

[2] L. F. McNamara, *The Ionosphere, Communications, Surveillance, and Direction Finding*, Melnourne, FL: Krieger Publishing, 1991.

[3] G. D. McNeal, "The high-frequency environment at the ROTHR Amchitka radar site," *Radio Science*, vol. 30, pp. 739–746, May–June 1995.

[4] L. Cohen, *Time-Frequency Analysis*, Englewood Cliffs, NJ: Prentice Hall, 1995.

[5] D. L. Jones and R. G. Baraniuk, "An adaptive optimal-kernel time-frequency representation," *IEEE Trans. Signal Processing*, vol. 43, no. 10, pp. 2361–2371, Oct. 1995.

[6] S. M. Kay, *Modern Spectral Estimation: Theory and Applications*, Englewood Cliffs, NJ: Prentice Hall, 1998.

[7] R. M. Nickel and W. J. Williams, "High resolution frequency tracking via non-negative time-frequency distributions," in *Proc. IEEE Workshop on Statistical Signal and Array processing*, Pocono, PA, Aug. 2000.